



## Prediction of Graphic Interaction Time of Virtual Reality System Based on Improved Fitts' Law

Zhenghong Liu<sup>1</sup>, Jian Lyu<sup>2</sup>, Huiliang Zhao<sup>3</sup>, Jie Liu<sup>1\*</sup>

<sup>1</sup> School of Mechanical Engineering, Guiyang University, Guiyang 550005, China

<sup>2</sup> Key Laboratory of Advanced Manufacturing Technology of the Ministry of Education, Guizhou University, Guiyang 550025, China

<sup>3</sup> Guizhou Minzu University, Guiyang 550025, China

Corresponding Author Email: [tomjie2008@126.com](mailto:tomjie2008@126.com)

<https://doi.org/10.18280/ts.370208>

### ABSTRACT

**Received:** 12 October 2019

**Accepted:** 8 February 2020

#### Keywords:

*virtual reality (VR), human computer interaction (HCI), Fitts' law, arbitrary shape*

This paper attempts to evaluate the click efficiency of different graphic designs of the virtual reality (VR) system for shipbuilding in a shipyard. For this purpose, a prediction method for the completion time of pointing tasks in a VR was proposed based on the probabilistic Fitts' law, and a selection model was constructed for targets in arbitrary shape in VR. According to the design requirements of VR interfaces, the authors considered the influence of target shape on task completion time, constructed the relationship between hit probability and the index of difficulty (ID) of the task, and took the target center as the center point of the function to be integrated, thus defining the probabilistic Fitts' model in VR scenes. Next, Experiment 1 was designed to compute the constant terms of probability function P(HIT) in the improved probabilistic Fitts' model; Experiment 2 was designed to calculate the constant terms of prediction function in the improved model. In this way, the improved probabilistic Fitts' model was completed. Finally, our model was validated and evaluated by the actual pointing task of the shipbuilding VR system of a shipyard. The results show that our model can predict the task completion time well under VR scenes. The research provides effective guidance for designers to optimize the interface layout in a VR environment, and optimize the user experience of interface interaction.

## 1. INTRODUCTION

The layout design of the interactive interface is based on the concept of humanized design. For two-dimensional (2D) interactive interfaces, the layout design, which mainly involves regular graphics, should emphasize the ease of use and aesthetics over the efficiency of interaction.

With the rapid development of artificial intelligence (AI), virtual reality (VR) has permeated into various aspects of our life, ranging from education, medical treatment to entertainment.

In the context of the VR, three-dimensional (3D) human-computer interaction (HCI) has become a basic operation over targets like menus, buttons, and texts. Rather than regular shapes (e.g. rectangle and circle), these targets are often irregular in shape.

Currently, most designers of irregular-shaped interactive interfaces only stress on the aesthetics of the layout, failing to consider the efficiency of interaction. In a VR system, however, high interaction efficiency is favored by users amidst an unfamiliar 3D environment.

The interaction efficiency is mainly measured by the interaction time under the effects of target geometry (e.g. shape, width, and height), and the cursor movement direction. Many scholars have attempted to evaluate the interaction efficiency of interfaces in a VR system.

For instance, Mackenzie and Buxton [1] derived two calculation models for the index of difficulty (DI) in acquiring

rectangular targets, namely, the size (W) model based on the approach angle and effective width of target, and the minimum model for the minimum size problem[2-4], and found that the models explain their experimental data well.

Accot and Zhai [5] found several problems with the above two models: the W model ignores the direction constraint, i.e. the influence of target size perpendicular to the moving direction; the minimum model is not affected by time, if the height of the target is greater than the width, and not affected by the width if the height is smaller than the width.

To overcome the problems, Accot and Zhai put forward the weighted Euclidean model, and verified that the proposed model outperforms the said two models. However, the weighted Euclidean model still does not consider all relevant factors of general 2D target acquisition tasks. For one thing, the movement angle is neglected, contrary to the conclusion of Hancock and Booth [6] that task completion time depends on the movement direction. For another, the weighted Euclidean model only tackles rectangular targets; it is unclear how to apply the model to targets with arbitrary width and height.

The above two limitations can be solved by the probabilistic Fitts' model proposed by Grossman and Balakrishnan [7]. This model applies to the direction modeling of targets with arbitrary shapes, a key difficulty in target acquisition. Grossman and Balakrishnan proved that the probabilistic Fitts' model can accurately predict the completion time of the pointing task of rectangular targets that differ in sizes, moving distances, and movement angles.

The Fitts' formula lays a good theoretical basis for the evaluation of interaction efficiency. For example, Thumser et al. adopted the Fitts' formula to calculate the target size during the gripping task using torque [8]. Lahib et al. relied on the Fitts' formula to measure and design the touch size of blind touch screen [9]. The Fitts' formula has also been improved to suit specific research goals. For instance, Murata and Fukunaga studied how moving direction influences the Fitts' formula under different target shapes, and developed an extended model based on the influence [10]. Drews et al. explored electronic health record on the go, and discovered that the task efficiency depends on the shape and size of the equipment [11]. Heath et al. found that the ratio of the ID and movement time (MT) (ID/MT) varies with the moving distance and target size, and that reducing the moving distance has greater impact on interaction time than increasing the target size [12]. Based on the Fitts' formula, You et al. examined the interaction efficiency of small target shapes in a VR environment [13].

Despite yielding fruitful results, the existing studies on the Fitts' formula mostly target flat graphical user interfaces, while few concentrate on the interactive interfaces in a VR environment. Moreover, there is virtually no report on irregular shaped interactive interfaces in a VR environment. To evaluate the interaction efficiency, it is important to build a better prediction model for the selection time of irregularly shaped targets in the HCI in a VR environment.

Therefore, this paper puts forward a model to acquire targets with arbitrary shapes in a VR environment, which can effectively predict the interaction time of users. The main contributions are as follows:

(1) The F function and the center of target shape of the Fitts' law were improved to suit the targets with arbitrary shapes in a VR environment.

(2) The authors proposed a method to calculate the value of the constant term in the probability function  $P(\text{Hit})$ , and designed Experiment 1 to ascertain the values of the constants  $c$  and  $d$ .

(3) An improved probabilistic Fitts' model was established by adding arbitrary target shapes and computing the constant term of the prediction function.

(4) A shipbuilding VR system was developed, and its HCI was used to verify the effectiveness of our model on the actual click tasks.

The remainder of this paper is organized as follows: Section 2 improves the Fitts' law; Section 3 obtains the probability function parameters  $c$  and  $d$  through Experiment 1; Section 4 calculates the prediction function parameters  $a$  and  $b$  through Experiment 2; Section 5 validates our model on actual cases; Section 6 puts forward the conclusions, and looks forward to future research.

## 2. IMPROVED FITTS' LAW

The Fitts' law is usually used to simulate the time consumption of target pointing tasks. The movement time MT1 of the cursor from any positive to the center of the target can be calculated by:

$$MT_1 = a + b \log_2 \left( \frac{A}{W} + 1 \right) \quad (1)$$

where,  $a$  and  $b$  are empirically constants;  $\log_2 \left( \frac{A}{W} + 1 \right)$  is the ID of the task;  $W$  is the size of the target;  $A$  is the hit range, i.e., the moving distance of the target. Obviously, MT1 is positively correlated with  $A$  and negatively with  $A$ .

According to Mac Kenzie et al., formula (1) can be used to predict the time of one-dimensional (1D) target pointing tasks, and also optimize the layout design of interfaces. From the perspective of interface designers, the Fitts' law is limited to 1D targets, while most targets in the user interface are 2D. To solve the problem, many scholars have extended the Fitts' law to two or higher-dimensional targets [14]. But the extensions only apply to 2D targets of regular shapes, such as rectangles and circles. In the VR environment, however, most interface designers want to model the pointing to targets of arbitrary shapes.

### 2.1 Probabilistic Fitts' model

The probabilistic Fitts' model has the potential to solve targets of any shape. The core idea is to map to probability of hitting a target using ballistic motion to the ID of the target. Ballistic motion is one of the two phases of the user's pointing motion during the HCI in a VR environment. The other phase is called the correction phase. In the ballistic phase, the user controls the cursor to move to the target point by turning the wrist. In the correction phase, the user needs to adjust the cursor with a high accuracy to capture the target. The correction phase occupies most of the time to complete the target pointing task.

Take the game of darts for example. If a dart is thrown towards the dartboard, it may fall close to or far away from the bullseye. After lots of darts have been thrown, the hit distribution can be adopted to predict the probability of hitting the bullseye or any other target on the dartboard. Similarly, the probability  $P$  (hit) of hitting the target without correction can be derived from the hit distribution  $S$  (formed by target or specific click area  $R$ ) using only ballistic motion and no correction. In the probabilistic Fitts' model, the probability  $P$  is mapped directly by the  $F$  function to the ID of the task:

$$ID_{Pr} = F(P_{R,S}(\text{hit})) \quad (2)$$

### 2.2 Improved F function

In order to determine the exact nature of function  $F$ , Grossman and Balakrishna examined the condition of 1D target, revealing that hit distribution obeys normal distribution. The mean of hit distribution equals zero, which corresponds to the center of the target. Hence, the  $ID_{Pr}$  of the task can be transformed into:

$$ID_{Pr} = F \left( P \left( -\frac{W}{2} \leq X_{N(0,\delta)} \leq \frac{W}{2} \right) \right) \quad (3)$$

where,  $X_{N(0,\delta)}$  is a random variable of the normal distribution with the mean of 0 and a standard deviation of  $\delta$ ;  $A$  is the distance from the current point to the target;  $W$  is the target width. The relationship between target and normal distribution is shown in Figure 1 below.

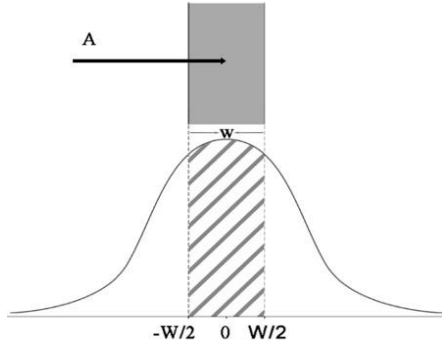


**Figure 1.** Relationship between target and normal distribution

In addition, the hit distribution  $S$  increases linearly with the amplitude  $A$  of cursor movement, because the hit range varies with the increase in target distance.

Going back to the dart game analogy, the points being hit are more scattered, as the darts fall further away from the bullseye. Then, the standard deviation  $\delta$  can be expressed as a function of  $A$ :  $\delta = kA$ . Therefore, the  $ID_{Pr}$  can be expressed as:

$$ID_{Pr} = F\left(P\left(-\frac{W}{2} \leq X_{N(0,kA)} \leq \frac{W}{2}\right)\right) \quad (4)$$

where,  $k$  is a constant empirically set to 0.07 [15]. The function  $F$  can be generated by replacing the left side of equation (4) with the ID of the traditional Fitts' law, and representing the right side as per the cumulative standard normal distribution:

$$\log_2\left(\frac{A}{W} + 1\right) = F\left(\Phi\left(\frac{W}{2kA}\right) - \Phi\left(-\frac{W}{2kA}\right)\right) \quad (5)$$

Since there is no closed formula for the cumulative normal distribution, the value of the function  $F$  can be calculated numerically by changing the  $A/W$  values in equation (5). The calculated results are displayed in Figure 2 below.

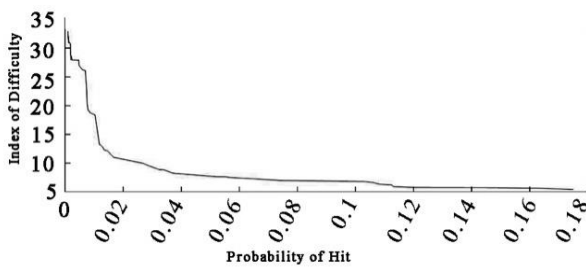


**Figure 2.** F function of  $k=0.07$

The ID of the task can be determined by calculating the probability of the ballistic motion hitting the target by the  $F$  function.

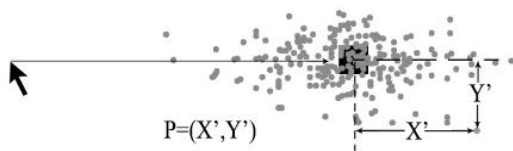


**Figure 3.** Hit distribution of 3D target pointing

For 2D target pointing, the hit point can be defined as point  $P=(X', Y')$ , where  $X'$  and  $Y'$  are the errors parallel and perpendicular to the moving direction, respectively (Figure 3). Then, the hit distribution can be modeled as a bivariate normal distribution  $N(\mu_x, \mu_y, \delta_x, \delta_y, \rho_{XY})$ . The mean  $(\mu_x, \mu_y)$  of the distribution equals zero, corresponding to the center of the target.

For some constants  $c$ , suppose the standard deviation fulfills  $\delta_x=cA$ , i.e. the distance measured from the center of the target, collinear with cursor movement direction.

For some constants  $d$ , suppose the standard deviation fulfills  $\delta_y=dA$ , i.e. the distance measured from the center of the target, perpendicular to the cursor movement direction.

$$bndf(X', Y') = \frac{1}{cA\sqrt{2\pi}} e^{-\left(\frac{X'^2}{2(cA)^2}\right)} \frac{1}{dA\sqrt{2\pi}} e^{-\left(\frac{Y'^2}{2(dA)^2}\right)} \quad (6)$$

Therefore, the ID of the 2D target pointing task can be calculated by:

$$ID_{Pr} = F\left(\iint_R bndf(X', Y') cX' dY'\right) \quad (7)$$

where,  $R$  is the target region; the brackets are the integrals of  $X'$  and  $Y'$  over  $R$ . Eq. (7) does not require the target to have a clearly defined height and width. The IDs of targets in any shape can be obtained by integrating over different regions  $R$ . Therefore, experiments need to be designed to determine the values of parameters  $c$  and  $d$ .

The improved prediction model can be finalized as:

$$MT = a + bID_{Pr} \quad (8)$$

### 2.3 Improved target center

Before applying the probabilistic Fitts' model to targets of any shape, it is important to determine the center of the target, that is, find the target area centered by the bivariate normal distribution.

The target center is the target point that the user is expected to hit initially. As shown in Figure 4, the center of the distribution function to be integrated is collinear with the target center. Therefore, positioning the target center will affect the performance of the probabilistic Fitts' model in two ways: the target center determines how the hit distribution overlaps the target, and also affects the standard deviation of the hit distribution, which is a function of the moving distance  $A$ .



**Figure 4.** Collinearity between the center of the distribution function and the target center

The target center was defined as the centroid of polygon: the mean of  $N(x_i, y_i)$ ,  $i=0, \dots, N-1$  vertices of the polygon.

First, area  $B$  of the polygon target was obtained through the standard calculation of polygon centroid:

$$B = \frac{1}{2} \sum_{i=0}^{N-1} (x_i y_{i+1} - x_{i+1} y_i) \quad (9)$$

Then, the target centroid  $(c_x, c_y)$  was defined as follows:

$$c_x = \frac{1}{6B} \sum_{i=0}^{N-1} (x_i + x_{i+1})(x_i y_i - x_{i+1} y_i) \quad (10)$$

$$c_y = \frac{1}{6B} \sum_{i=0}^{N-1} (y_i + y_{i+1})(x_i y_{i+1} - x_{i+1} y_i) \quad (11)$$

### 3. PROBABILITY FUNCTION PARAMETERS

Experiment 1 was designed to study the hit distribution of ballistic pointing motion. The experimental results were used to determine constants  $c$  and  $d$  in equation (6).

#### 3.1 Instruments and subjects

In Experiment 1, 3D modelling was carried out on Rhinoceros under a scene built on the Unreal Engine 4 blueprint. The HTC Vive was taken as the input device. According to *The Research Report on China VR User Behavior* released in early 2016, the VR users in China are mainly aged between 20 and 40. Therefore, 10 students (including 1 female) between 18 and 30 were selected for Experiment 1. Only one of them is left-handed.

#### 3.2 Experimental design

Based on Kopper's research, three rectangular targets were selected, whose widths ( $W$ ) are 0.01m, 0.015m and 0.020m, respectively. Three movement amplitudes  $A(0.2758m, 1.379m, 2.04822m)$  and five movement angles  $\theta(0^\circ, 22.5^\circ, 45^\circ, 67.5^\circ, 90^\circ)$  were adopted.

Stefels et al. held that the distance between the user and the interactive interface is an important factor affecting the task performance [16]. Previous experiments show that the optimal distance between the user and the interactive interface is 1.52m. Therefore, the distance between the subject and the virtual interactive interface was set to 1.52m.

Through full orthogonal design, a total of 45 parameter combinations were produced, each of which contains 20 clicks from the starting point to the target.

Before each experiment, the subject was asked to get familiar with the task in 2min. For each subject, it took about 25min to complete the tasks.

#### 3.3 Experiment procedure



Figure 5. Repeated clicks on green and yellow targets

Before the experiment, the subject must read the instructions, and then click on the target quickly. During the experiment, only two targets appeared on the screen. The first target is green and the last target is yellow. Once the green target was selected, the green target changed color, prompting the subject to select the yellow target. As shown in Figure 5, this process was repeated continuously.

#### 3.4 Experimental results

Outliers were removed based on MT and precision. Any data that exceeds its conditional mean by 2 standard deviations was removed. In total, about 5% of experimental data were identified as outliers and deleted. To obtain  $c$  and  $d$  in the model, it is assumed that  $\delta_{x'} = cA, \delta_{y'} = dA$ . On this basis, a linear regression without intercept was performed for each movement angle  $\theta$ . The results are recorded in Table 1.

Table 1. Linear regression results of each movement angle  $\theta$

	c		R <sup>2</sup>	d		R <sup>2</sup>
	Estim	Std.Er		Estim	Std.Er	
0°	0.0717	0.0018	0.998	0.0284	0.0046	0.9243
22.5°	0.0686	0.0027	0.995	0.0304	0.0043	0.9413
45°	0.0634	0.0047	0.984	0.0344	0.0061	0.9117
67.5°	0.0582	0.0071	0.957	0.0331	0.0035	0.9668
90°	0.0665	0.0028	0.995	0.0345	0.0078	0.861

#### 3.5 Sample calculation

Based on the empirically determined values of  $c$  and  $d$ , the  $ID_{Pr}$  value of the 2D target pointing was computed under the experimental conditions. Take a right triangle with  $A=1.3729m$ ,  $W=0.015m$ , and  $\theta=0^\circ$  as an example (Figure 6). Substituting these values into Eq. (7), the integration area can be determined by the target width  $W$  to obtain:

$$ID_{Pr} = F \left( \frac{\int_{-0.0105}^{0.0045} \int_{-0.0045}^{X'+0.006} \frac{1}{0.0717 \times 1.3729 \sqrt{2\pi}} e^{-\left(\frac{X'^2}{2 \times (0.0717 \times 1.3729)^2}\right)} \frac{1}{0.0284 \times 1.3729 \sqrt{2\pi}} e^{-\left(\frac{Y'^2}{2 \times (0.0284 \times 1.3729)^2}\right)} dX' dY' \right)$$

With MATLAB, it can be solved that  $ID=(0.0552)_{pr}$ .

Then,  $F(0.0552)$  was searched for in the list of the IDs at different  $A/W$  values (Table 2). Linear interpolation was performed between  $F(0.055217)$  and  $F(0.05469)$  to obtain the desired  $ID_{Pr}$  value. The results are plotted as Figure 7.

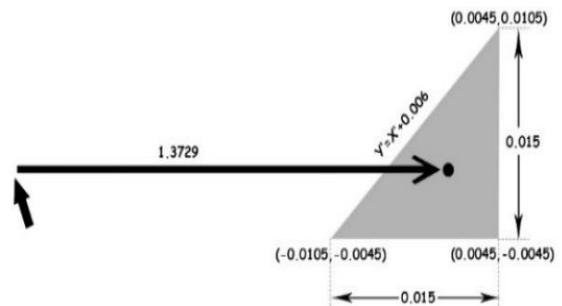
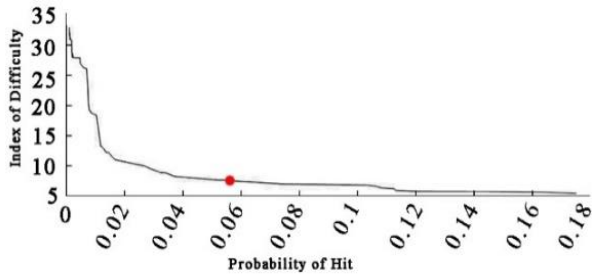


Figure 6. Acquisition of a right triangle-shaped target

**Table 2.**  $ID_{Pr}$  calculated by equation 5 for different A/W

(A/W)	P(Hit)	$ID_{Pr}$
...	...	...
98.2	0.055217	7.413
98.3	0.05469	7.522
...	...	...
...	...	...



**Figure 7.** Example of calculating F (0.05469)  $ID_{Pr}=7.416$

The IDs of other movement angles were calculated similarly. Take a rectangular target with  $A=1.3729$ ,  $W=0.015$ , and  $\theta=67.5^\circ$  as an example. The distribution of the cursor click points was also rotated. The hits were assumed to follow a binary normal distribution, which rotated  $67.5^\circ$  (shown in Figure 8a). The attributes of the target were still  $A=1.3729$ ,  $W=0.015$ , and  $\theta=0^\circ$ , but with a  $-67.5^\circ$  rotation on the defined area R (Figure 8b). In this case, the c and d in Experiment 1 are applicable, but the integration area had changed.

Therefore, the ID can be calculated as:

$$ID_{Pr} = F \left( \frac{\iint_R \frac{1}{0.0717 \times 1.3729 \sqrt{2\pi}} e^{-\frac{x^2}{2 \times (0.0717 \times 1.3729)^2}}}{\frac{1}{0.0284 \times 1.3729 \sqrt{2\pi}} e^{-\frac{y^2}{2 \times (0.0284 \times 1.3729)^2}}} dX' dY' \right)$$

With MATLAB, it can be solved that  $ID=(0.248)_{Pr}$ , i.e.  $ID=4.519_{Pr}$ .

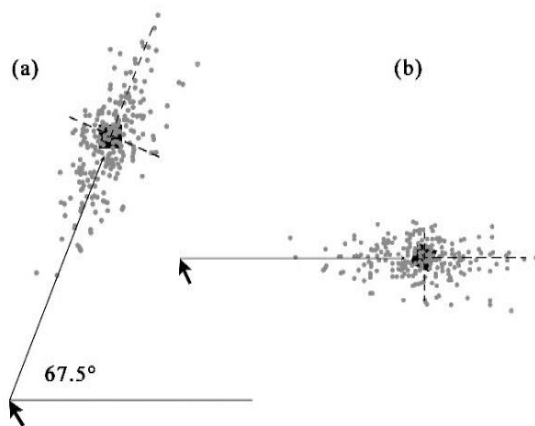


**Figure 8.** (a) Integrating the bivariate normal distribution rotated by  $67.5^\circ$  over the region defined by a rectangle. (b) Integrating the nonrotated bivariate normal distribution over the region defined by a rectangle rotated by  $-67.5^\circ$

## 4. PREDICTION FUNCTION PARAMETERS

Experiment 2 was designed based on Experiment 1, and the target shape was treated as an independent variable. Then, the constant term of the improved probabilistic Fitts' model was calculated.

### 4.1 Experimental design

Experiment 2 aims to judge whether the improved probabilistic Fitts' model is suitable for targets of any shape in the VR environment, rather than compare the motion time of different shapes. If proved suitable, the model could be used to predict whether a target of a specific size and shape is easier to select than that of another size and shape.

Drawing on relevant literature of computer vision [17], targets of six classic shapes (Figure 9) were selected to test the improved probabilistic Fitts' model.

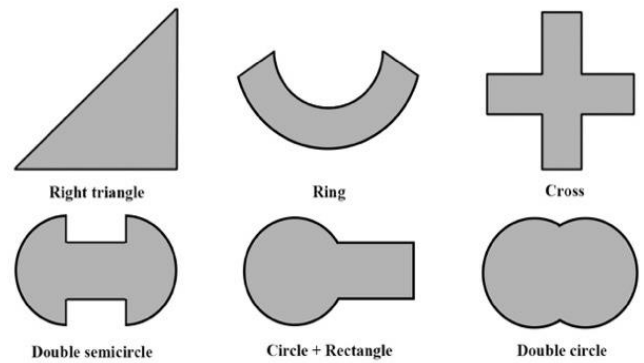


**Figure 9.** The six shapes used in Experiment 2

Then, three target widths  $W(0.010m, 0.015m, 0.020m)$ , three movement amplitudes  $A(0.2758m, 1.379m, 2.4822m)$ , and 5 movement angles  $\theta(0^\circ, 22.5^\circ, 45^\circ, 67.5^\circ, 90^\circ)$  were chosen for the experiment. The movement amplitude, the movement angle, the target size, and the target shape were taken as independent variables, while task completion time was taken as the dependent variable.

During the experiment, the subject always stood on a right-angled extension line 1.52m from the center of the virtual interactive interface. The experiment started once the subject clicked on the first target, and ended when the subject clicked on the second target. The task completion time was measured by a timekeeping software (accurate to three decimal places).

Three movement amplitudes were presented in artificially balanced order, aiming to avoid the delay from the initial position to the target position due to exercise fatigue. The subject repeatedly clicked 20 times on 180 parameter combinations, producing a total of 36,000 sample data.

After completing a task, the subject took a 5s-long rest for the next task, such as to avoid errors from motion inertia. Before each experiment, the subject was asked to get familiar with the task in 5min. For each subject, it took about 50min to complete the tasks.

### 4.2 Experimental results

Among the experimental data, 3.9% were time outliers resulted from timer delay and other reasons. These data were considered invalid, and directly removed.

Through repeated measures analysis of variances

(ANOVA), it is learned that target shape ( $F_9, 81=214, p<.000$ ), target size ( $F_2, 18=6092, p<.0001$ ), and movement amplitude ( $F_2, 18=10934, p<.0001$ ) were the main influencing factors. The moving distance and target size can be predicted from the original Fitts' formula; the target shape also has a significant impact on the task completion time, indicating that the ID varies with the target shape. This further validates that the target shape must be included in the prediction model. Figure 10 shows the task completion time for targets of six shapes in different sizes and amplitudes.

The target center of each shape should be defined before evaluating the experimental data. Figure 11 shows the target center of each shape with  $A=2.4822m$  and  $W=20cm$ .

A probabilistic Fitts' model was used to calculate the  $ID_{Pr}$  for each parameter combination (Tables 3a and 3b) by equation (7), where the integration region R is a target shape.

Next, MATLAB Curve Fitting Toolbox was called to solve equation (8) for linear regression analysis, and the results were plotted as Figure 12.

The determination coefficients include  $SSE=0.0627$ ,  $R^2=0.9488$ , intercept  $a=0.2788$ , and slope  $b=0.01472$ . Therefore, the final improved prediction model can be expressed as:

$$MT = 0.2788 + 0.01472ID_{Pr} \quad (12)$$

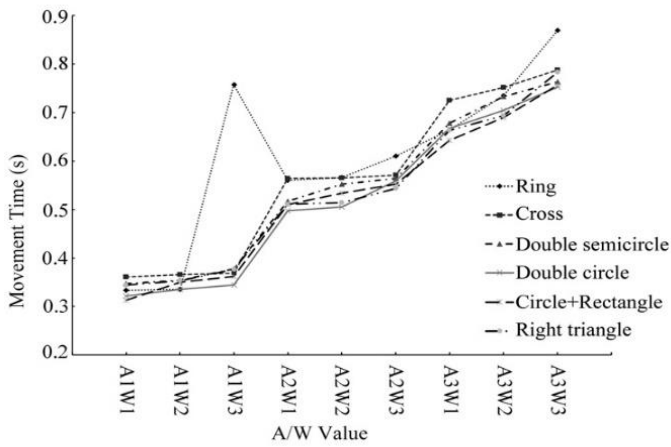


Figure 10. Task completion time for targets of six shapes in different sizes and amplitudes.

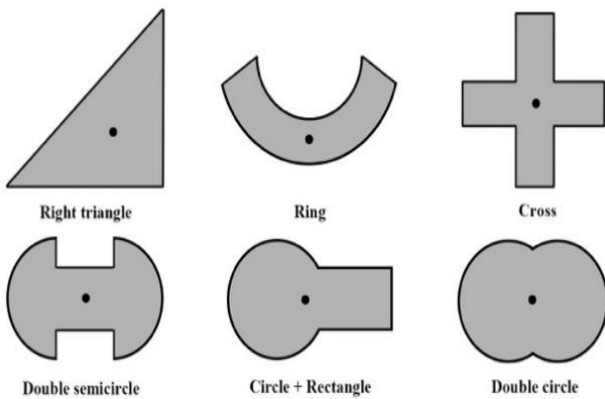


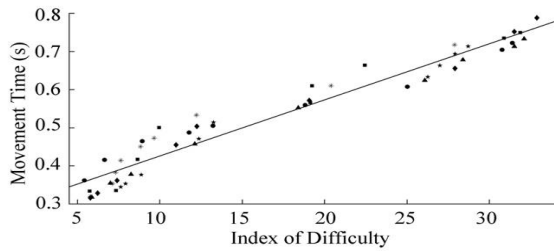
Figure 11. The target center of each shape

Table 3a.  $ID_{Pr}$  under different shapes, amplitudes and sizes

Shape	(W/A)	P(Hit)	$ID_{Pr}=F(P)$	
Double semicircle	0.7252	0.0939	6.882	
	0.5439	0.0741	7.013	
	0.3626	0.0371	8.265	
	0.145	0.0147	12.134	
	0.1088	0.0103	18.414	
	0.0806	0.00699	26.092	
	0.0725	0.00221	28.406	
	0.0604	0.00114	32.121	
	0.0403	0.001	31.529	
	Right triangle	0.7252	0.0552	7.641
		0.145	0.05	7.931
		0.0806	0.0324	8.883
0.5439		0.0134	12.379	
0.1088		0.0118	13.268	
0.0604		0.0059	26.274	
0.3626		0.0048	27.004	
0.0725		0.0024	27.93	
0.0403		0.002	28.722	
Ring		0.7252	0.1433	5.754
		0.145	0.1084	6.355
		0.0806	0.106	6.654
	0.5439	0.0269	9.962	
	0.1088	0.00807	19.144	
	0.0604	0.00789	19.259	
	0.3626	0.00746	22.446	
	0.0725	0.00141	30.897	
	0.0403	0.0012	30.897	

Table 3b.  $ID_{Pr}$  under different shapes, amplitudes and sizes

Shape	(W/A)	P(Hit)	$ID_{Pr}=F(P)$	
Circle + rectangle	0.7252	0.103	6.823	
	0.145	0.0633	7.341	
	0.0806	0.0564	7.531	
	0.5439	0.0519	7.657	
	0.1088	0.034	8.846	
	0.0604	0.0282	9.66	
	0.3626	0.0144	12.236	
	0.0725	0.00758	20.413	
	0.0403	0.00473	27.898	
	Double circle	0.7252	0.175	5.431
		0.145	0.163	5.656
		0.0806	0.113	5.944
0.5439		0.013	12.786	
0.1088		0.0121	13.236	
0.0604		0.00847	18.831	
0.3626		0.0019	29.035	
0.0725		0.0018	30.783	
0.0403		0.0013	31.405	
Cross		0.7252	0.12	5.791
		0.145	0.1125	6.236
		0.0806	0.0601	7.416
	0.5439	0.0167	11.005	
	0.1088	0.0137	12.268	
	0.0604	0.00838	19.092	
	0.3626	0.002	27.93	
	0.0725	0.0012	31.529	
	0.0403	0.001	32.898	



**Figure 12.** The scatterplot of task completion time at 12 different  $ID_{Pr}$  values

## 5. EXAMPLE VERIFICATION

In the VR environment, the HCI involves direction tasks like input and target selection. Most HIC interface designers focus too much on their own feelings. The scenes designed by them are poor in user experience, rationality, and persuasiveness.

To verify its effectiveness, our model was adopted to predict the task completion time based on the target shape, target size, and movement amplitude, and the prediction was compared with the actual task completion time.

For this purpose, a VR shipyard system was developed based on Unreal Engine 4 blueprint. Taking HTC Vive as the input device, the proposed system was positioned in a VR environment and further customized (Figure 13).



**Figure 13.** VR shipyard system

### 5.1 Verification experiment

During the experiment, 8 right-handed subjects aged 20-30 were selected, 4 of whom had good VR experience (denoted as *A*, *B*, *C*, and *D*), and the other 4 had general VR experience (denoted as *E*, *F*, *G*, and *H*). Five existing VR HCI interfaces were integrated to the experimental interface. As shown in Figure 14, the experimental interface is  $1,200 * 500mm$  in size; the subject performed pointing from the interface elements 1-6 in order. Once a target element is selected, the target color became purple. The MT required to complete the task was recorded in real time.



**Figure 14.** The experimental interface

## 5.2 Results analysis

The experimental data were sorted for analysis. Table 4 shows the mean task completion time MT for skilled and average testers in VR operation. The task completion time MT predicted by the improved probabilistic Fitts' model was compared with the MT against two statistical metrics Euclidean distance and Kullback-Leibler (KL) divergence. By the two metrics, the mean accuracy of our predictions was 80.0241% and 84.8751%, respectively. It shows that the improved model can effectively predict the completion time of target pointing tasks.

**Table 4.** The mean task completion time and predicted time of eight subjects for each of the five interface elements

MT	1	2	3	4	5
A	0.71	0.51	0.62	0.68	0.82
B	0.68	0.47	0.71	0.64	0.65
C	0.81	0.72	0.76	0.76	0.77
D	1.05	0.69	0.85	0.92	0.92
E	1.31	0.95	1.04	1.18	1.26
F	1.16	0.906	1.053	0.949	1.139
G	1.34	1.012	1.099	1.236	1.229
H	0.87	0.584	0.761	0.841	0.895
MT'	0.994	0.732	0.864	0.904	0.962

## 6. CONCLUSIONS

In a VR environment, targets may have arbitrary shapes. Therefore, this paper designs a model that can effectively predict the task completion time of the target of arbitrary shapes in the context of the VR. Based on the probabilistic Fitts' law, the model was designed based on the analysis of experimental data. The model includes several factors that affect task performance, namely, moving distance, target size, target shape, and movement angle.

The main work is summarized as follows: (1) an improved Fitts' law was proposed to define the ID by the F function and to calculate the center of target in any shape. (2) An experiment was designed to calculate constants *c* and *d*, making it possible to obtain the probability of hitting the target without correction, and ascertain the ID of the pointing task. (3) The target shape was included as an independent variable, different target shapes were tested, and the constants *a* and *b* were calculated in the prediction function, thereby setting up the prediction model. (4) The validity and accuracy of our model were verified through a case study. The results show that the mean prediction accuracy of the model was as high as 80.0241%. Our model provides guidance for the design of HCI interfaces in a VR environment, and offers a reference for the evaluation of design plans.

The future research will focus on two aspects: (1) The prediction accuracy of our model was verified with 5 VR HCI interfaces. To further test the accuracy, more interfaces in different shapes will be selected for verification experiments. (2) In the future, our model will be optimized for dynamic target pointing in VR scenes.

## ACKNOWLEDGEMENTS

This work was supported by the National Natural Science Foundation of China (Grant No.: [2017]239 and [2018]152),

the Special Funding of Guiyang Science and Technology Bureau and Guiyang University (Grant No.: GYU-KYZ (2019~2020) JX-02), the Guizhou Provincial Colleges and Universities Auto Service Technology Industry-university-research Base Project (Grant No.: 20190365101), the Guizhou Province First-class University 2017-first-class Teaching Platform Construction Project (Grant No.: 2018052510103), The Ministry of Education First Batch of "New Engineering" Research and Practice Project (Grant No.: 20190205103), and the Guizhou Provincial Department of Education College Student Innovation and Entrepreneurship Training Center Construction Project (Grant No.: 20180255102).

## REFERENCES

- [1] Mackenzie, I., Buxton, W. (1992). Extending Fitts' law to two-dimensional tasks. *ACM*, 1992: 219-226. <https://doi.org/10.1145/142750.142794>
- [2] Ware, C., Balakrishnan, R. (1994). Reaching for objects in VR displays: Lag and frame rate. *ACM Transactions on Computer-Human Interaction*, 1(4): 331-356. <https://doi.org/10.1145/198425.198426>
- [3] Ware, C., Lowther, K. (1997). Selection using a one-eyed cursor in a fish tank VR environment. *ACM Transactions on Computer-Human Interaction*, 4(4): 309-322. <https://doi.org/10.1145/267135.267136>
- [4] Iwase, H., Murata, A., Kitaoka, M., Balingit, J. (2011). Improvement of the model of Fitts' law in a two-dimensional pointing task. *Critical Quarterly*, 40(9): 881-889. <https://doi.org/10.1111/j.1467-8705.2011.00039.x>
- [5] Accot, J., Zhai, S. (2003). Refining Fitts' law models for bivariate pointing. *ACM*, 2003: 193-200. <https://doi.org/10.1145/642611.642646>
- [6] Hancock, M.S., Booth, K.S. (2009). Improving menu placement strategies for pen input. *Proceedings of the Graphics Interface 2004 Conference*, London, Ontario, Canada, pp. 221-230.
- [7] Grossman, T., Balakrishnan, R. (2005). The bubble cursor: enhancing target acquisition by dynamic resizing of the cursor's activation area. *Proceedings of the 2005 Conference on Human Factors in Computing Systems, CHI 2005*, Portland, Oregon, USA, 12(3): 435-459. <https://doi.org/10.1145/1054972.1055012>
- [8] Thumser, Z.C., Slifkin, A.B., Beckler, D.T., Marasco, P.D. (2018). Fitts' law in the control of isometric grip force with naturalistic targets. *Frontiers in Psychology*, 9: 560. <https://doi.org/10.3389/fpsyg.2018.00560>
- [9] Lahib, M.E., Tekli, J., Issa, Y.B. (2018). Evaluating Fitts' law on vibrating touch-screen to improve visual data accessibility for blind users. *International Journal of Human Computer Studies*, 112: 16-27. <https://doi.org/10.1016/j.ijhcs.2018.01.005>
- [10] Murata, A., Fukunaga, D. (2018). Extended Fitts' model of pointing time in eye-gaze input system-incorporating effects of target shape and movement direction into modeling. *Applied Ergonomics*, 68: 54-60. <https://doi.org/10.1016/j.apergo.2017.10.019>
- [11] Drews, F.A., Zadra, J.R., Gleed, J. (2018). Electronic health record on the go: device form factor and Fitts' law. *International Journal of Medical Informatics*, 111: 37-44. <https://doi.org/10.1016/j.ijmedinf.2017.12.010>
- [12] Heath, M., Samani, A., Tremblay, L., Elliott, D. (2016). Fitts' theorem in oculomotor control: Dissociable movement times for amplitude and width manipulations. *Journal of Motor Behavior*, 48(6): 1-11. <https://doi.org/10.1080/00222895.2015.1134436>
- [13] You, Q., Lv, J., Li, Y., Jin, Y.T., Zhao, Z.J. (2019). Small target selection model in virtual reality based on Fitts' law. *Chinese Journal of Engineering Design*, 26(4): 416-422. <https://doi.org/10.3785/j.issn.1006-754X.2019.04.007>
- [14] Deng, C., Geng, P., Hu, Y.F., Kuai, S.G. (2019). Beyond Fitts's law: a three-phase model predicts movement time to position an object in an Immersive 3D virtual environment. *The Journal of the Human Factors and Ergonomics Society*, 61(6): 879-894. <https://doi.org/10.1177/0018720819831517>
- [15] Grossman, T., Balakrishnan, R. (2005). The bubble cursor: Enhancing target acquisition by dynamic resizing of the cursor's activation area. *Proceedings of the 2005 Conference on Human Factors in Computing Systems, CHI 2005*, Portland, Oregon, USA, pp. 281-290. <https://doi.org/10.1145/1054972.1055012>
- [16] Stefels, C.N., Kneissner, J., Aarnink, R.G., Kaufholz, P., Grimbergen, C.A., Dankelman, J. (2009). Equipment control in a sterile environment using the gyro mouse and a new interface, the user interface (UI) wand. *Minimally Invasive Therapy & Allied Technologies*, 16(3): 163-172. <https://doi.org/10.1080/13645700701384157>
- [17] Wang, W.G., Shen, J.B., Jia, Y.D. (2019). Review of visual attention detection. *Journal of Software*, 30(2): 416-439. <https://doi.org/10.13328/j.cnki.jos.005636>



Copyright of Traitement du Signal is the property of International Information & Engineering Technology Association (IIETA) and its content may not be copied or emailed to multiple sites or posted to a listserv without the copyright holder's express written permission. However, users may print, download, or email articles for individual use.